Talanta 134 (2015) 568–575

Contents lists available at ScienceDirect

Talanta

journal homepage: www.elsevier.com/locate/talanta

Plasmonic detection of Cd^{2+} ions using surface-enhanced Raman scattering active core–shell nanocomposite

Sheenam Thatai [a], Parul Khurana [a], Surendra Prasad [b,*], Dinesh Kumar [a,**]

[a] Department of Chemistry, Banasthali Vidyapith, Banasthali 304022, Rajasthan, India
[b] School of Biological and Chemical Sciences, Faculty of Science, Technology and Environment, The University of the South Pacific, Private Mail Bag, Suva, Fiji

ARTICLE INFO

Article history:
Received 5 July 2014
Received in revised form
11 November 2014
Accepted 12 November 2014
Available online 20 November 2014

Keywords:
Au nanoparticles
Cd^{2+} ions sensor
Electron microscopy
Selectivity
Surface plasmon resonance
SERS active

ABSTRACT

The present study was structured to address development of an efficient devise for sensing of toxic Cd^{2+} ions at trace level in aqueous media. In order to achieve this objective, the speckled core–shell nanocomposites (NCs) of silica-gold (SiO_2@Au) using ~30 nm diameter of spherical gold nanoparticles (Au NPs) with 420 nm diameter of silica cores was synthesized. Au NPs showed the surface plasmon resonance (SPR) peak at 522 nm and spherical core–shell particles at 541 nm. Both Au NPs and SiO_2@Au solutions were found to be sensitive to Cd^{2+} ions in aqueous sample. The colour change occurred in presence of SiO_2@Au at 0.1 ppm (100 ppb) of Cd^{2+} ions whereas 2 ppm (2000 ppb) concentration of Cd^{2+} ions was necessary for the colour change in Au NPs solution confirmed that SERS active SiO_2@Au core–shell NCs 20 times more sensitive compared to Au NPs. The technique using SiO_2@Au NCs is quantitative between 100 and 2000 ppb (0.1 to 2 ppm) while effective but non-quantitative above upto 10 ppm, the maximum concentration studied in present investigation. The detection limit using SiO_2@Au NCs is 100 ppb (0.1 ppm) while Au NPs is able to detect Cd^{2+} as low as 2000 ppb (2 ppm). The scanning electron microscopy (SEM) of Au NPs and SiO_2@Au particles showed aggregation of Au NPs and SiO_2@Au NCs in the presence of Cd^{2+} ions. The surface enhanced Raman spectroscopy (SERS) was used to compare sensitivities of Au NPs and SiO_2@Au towards Cd^{2+} ions and confirmed that SiO_2@Au core–shell NCs is 20 times more sensitive than Au NPs.

1. Introduction

The exposure to heavy metals like cadmium, mercury, lead, chromium, arsenic etc. through drinking water is not uncommon, more so due to contamination from industrial effluents. Industrial waste water, particularly with dissolved heavy metal ions like those of Cd, Hg, Pb, Cr, As, etc., has thus been of a great concern due to health hazards they cause to humans, aquatic animals as well as environmental damage [1,2]. Water contamination with heavy metal ions from a variety of industries is often found in many industrialized zones. The absorption of such water in the soil consequently contaminates the agricultural products, consumption of which can be dangerous in the long run [3,4]. Slow accumulation of heavy metal ions in human bodies is known to cause cancer, bone fracture, fast aging, etc. Therefore, development of sensitive and selective method to detect and determine trace levels of toxic metals is necessary and is of public interest [5].

Cadmium is a heavy metal and can enter water and subsequently soil mainly due to industries. Kidneys, due to their ability to reabsorb and accumulate, are the first target organ of metal toxicity upon chronic exposure [6]. Chronic cadmium toxicity leads to nephropathies, with various levels of severity ranging from tubulo-interstitial disease to end stage renal disease (ESRD) and to death [7]. Therefore cadmium is considered a priority pollutant by the European Community, within the Water Framework Directive [8,9], USA Environmental Protection Agency [8,10], United Nations Environment Programme, 2010, and also included in the OSPAR (Oslo Paris Convention) Commission's list of chemicals for priority action [9,11]. It is hazardous to human health as it causes severe stomach pain, diarrhoea, bone fracture, damage to central nervous system, cancer development, etc. Therefore, urgent social need to detect Cd^{2+} ions in water is very important.

In recent years with the developments in the field of nanotechnology, a variety of functional nanomaterials (NMs) like metal and metal oxide nanoparticles (NPs), quantum dots, carbon nanotubes, graphene, core–shell particles, etc. have been synthesized for the applications in various fields such as electronics, structural materials, textile, biology, aerospace, automobile and agriculture [12]. High efficiency, cost effectiveness and in many cases simple synthesis procedures make NMs an alternative choice

* Corresponding author. Tel.: +679 3232416; fax: +679 2321512.
** Corresponding author. Tel.: +91 9928108023; fax: +91 1438 228365.
E-mail addresses: prasad_su@usp.ac.fj (S. Prasad), dsbchoudhary2002@gmail.com (D. Kumar).

http://dx.doi.org/10.1016/j.talanta.2014.11.024
0039-9140/

over the conventional bulk materials for environmental remediation [13]. Nanomaterials are very useful particularly in the field of sensing of heavy metal ions as NMs have large surface to volume ratio which is available for interaction with chemical species of interest as compared to micro or bulk materials [5,12,13]. Therefore, NMs have enabled the detection as well as quantitative determination of chemical species in biological, chemical, environmental, food, physical as well as geological samples [5,12–22].

There are reports dealing with the detection of toxic metal ions using NPs [5,12–22] and the most recent review on the subject with 270 references has been published by us [23]. In most of these applications spectral changes occur due to aggregation of probing NPs in the presence of metal ions. Colorimetric changes have also been shown to occur in presence of metal NPs [17,19,21–23]. Therefore, colorimetric sensors detect the changes in colour on interaction of metal ions with NPs making them very useful as they do not require costly or complicated equipment or highly trained manpower for their operation and use. However, NPs used in many cases have been functionalized using complicated molecules or protocols [5,18,22,23]. Therefore there is still a need to improve the sensitivity and selectivity to detect the toxic metal ions in water using simple NPs synthesis as well as less expensive and easy to use colorimetric tests.

Recently nanoparticles have successfully been replaced by core–shell particles in order to confine the charges, protect the sensitive particles using inert material shell, increase the surface area keeping the advantages of 'nano size' by using inert core and thin shell or epitaxially making core–shell particles for desired structure [23–33]. This has led to the development of varieties of core–shell particles, reported in the literature, from few nanometers to hundreds of nanometer size depending on the applications like biosensing, drug delivery, imaging, cancer therapy or photonic band gap structures [23,24,30,33–36]. Thus the core–shell particles of metal-silica have also been reported [23,37–39]. Some core–shell particles synthesized and used have been referred to as '*speckled*' silica-gold core–shell nanocomposites (SGCSNCs) because they appear as tiny 'specks' on large smooth silica particles used as a core [40]. Silica-gold composites show 'nanogaps' between them which provide room for accommodation of metal ions as '*the hot spots*' leading to better sensitivity [41,42]. Hot spots may be attributed to enhanced electromagnetic field at the nano-tips of particles [39,40,42]. Thus surface enhanced Raman scattering (SERS) and the surface plasmon resonance (SPR) have emerged as a sustainable for non-invasive and bio-friendly analytical techniques for the detection of chemical, environmental and biological materials and have often been used as the mechanism behind the sensing action [23,42]. In recent years SERS is one of the most widely exploited properties for sensing application [23,25–29,37,41–52] and promises to be one of the most useful techniques for future applications in sensing as well as diagnosis. Therefore in our continued research interest in developing analytical methods for various analytes [23,37,43,53–62], the present communication reports our developed method for the detection of Cd^{2+} ions in water samples using SERS active SiO_2@Au core–shell nanocomposites (NCs). To the best of our knowledge no studies on the detection of Cd^{2+} ions based on SERS active SiO_2@Au core–shell NCs. For comparing the performance of NPs with core–shell particles herein we have also used both Au NPs and SiO_2@Au nanocomposites for the detection of Cd^{2+} ions in water.

2. Experimental

2.1. Materials

All reagents used were of analytical grade. Tetraethyl orthosilicate (TEOS), ethanol ($\geq$ 99.5%), ammonium hydroxide (NH_4OH, $\geq$ 25% w/v in H_2O), tetrachloroaurate(III) dihydrate ($HAuCl_4 \cdot 2H_2O$), sodium borohydride ($NaBH_4$), trisodium citrate dihydrate ($Na_3C_6H_5O_7 \cdot 2H_2O$), 3-aminopropyltriethoxysilane (APTES), potassium carbonate (K_2CO_3), cadmium(II) acetate dihydrate [$Cd(CH_3CO_2)_2 \cdot 2H_2O$], and crystal voilet (CV) molecule were procured from Sigma-Aldrich (USA). Indium tin oxide (ITO) slides were also obtained from Sigma-Aldrich and used as such. All these chemicals were used without further purification. Triple distilled de-ionized water was used throughout the experiments. All the glassware were cleaned by freshly prepared aqua regia and rinsed with distilled water in all the experiments.

2.2. Synthesis of gold nanoparticles

The Au NPs were synthesized by colloidal reduction method [63,64]. Trisodium citrate (5 mL of 0.03 M) was added to the boiling $HAuCl_4 \cdot 2H_2O$ aqueous solution (10 mL of 5 mM) while stirring under reflux. The reaction mixture was kept boiling for about 30 min where deep wine red colour was observed, indicating the formation of Au NPs. The heating mantle was turned off leaving the water condenser on until the NPs solution cooled down to 25 °C. The Au NPs were isolated from the colloidal solution by centrifugation at 4000 rpm for 30 min, **w**ashed three times with 8 mL de-ionised water. The NPs thus obtained were dispersed in Millipore water for further use. TEM and SEM measurements showed that the mean diameter of the synthesized Au NPs was about 30 nm.

2.3. Synthesis of SiO_2 nanoparticles

Silica nanoparticles were synthesized using the Stöber et al. method with minor modifications as outlined in Scheme 1 [65]. Ethanol (15 mL), water (3 mL) and NH_4OH (0.75 mL) were mixed in a round bottom flask (RBF) at 25 °C and stirred for 30 min. To this solution, 1.2 mL tetraethyl orthosilicate (TEOS) was added and the solution was further stirred for 3 h. A white precipitate of SiO_2 particles was obtained which was thoroughly washed with ethanol several times and dried. XL30 scanning electron microscope (SEM) was used to characterize SiO_2 particles size and was found to be 420 nm in diameter.

2.4. Synthesis of SiO_2@Au nanocomposites

In order to synthesize SiO_2@Au nanocomposites (NCs), the silica particles were initially functionalized using 3-aminopropyltriethoxysilane (APTES) as binder. An APTES molecules has one OH end and the other end has NH_2 group. Therefore, it can bond to silica

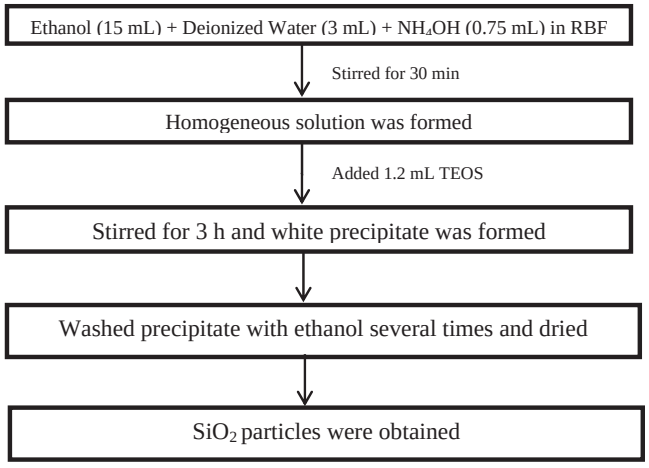

Scheme 1. Scheme showing the synthesis of silica nanoparticles.

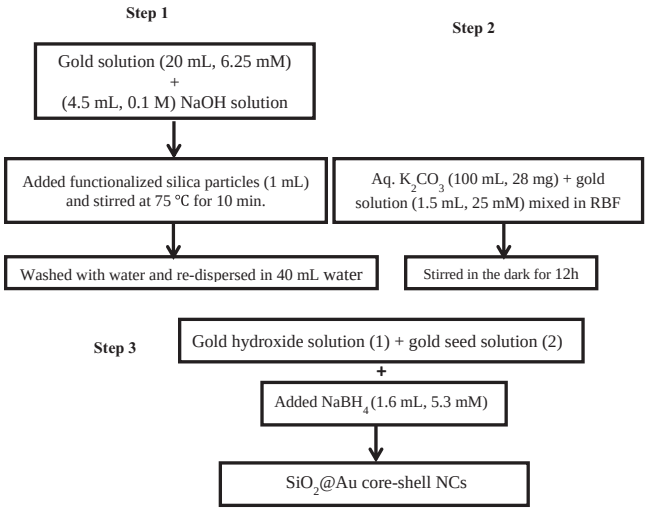

Scheme 2. Synthesis of core–shell nanocomposites in three step process. Step 1: Formation of gold seeds with silica particles by adding gold solution with sodium hydroxide and functionalized silica particles. Step 2 is the preparation of gold seed solution. Step 3 is the mixing of solution (1) and (2) from step 1 and step 2 respectively to obtain speckled gold SiO_2@Au nanocomposites.

through O and gold via N atoms. The functionalization of silica particles was performed using 12 mM APTES in C_2H_5OH:H_2O (3:1 v/v) and adding silica particles (0.04 mg in 4 mL) to it with APTES: silica (2.3:1 v/v). The resulting solution was vigorously stirred at 75°C for 4 h. The solution was centrifuged and the precipitate was washed with water. The functionalized silica particles were then re-dispersed in water. Thereafter speckled SiO_2@Au core–shell composites were synthesized in a three step procedure as shown in Scheme 2 [16,38].

In step 1, 20 mL (6.25 mM) of gold ($HAuCl_4 \cdot 2H_2O$) solution was mixed to 4.5 mL (0.1 M) of NaOH solution where pH 7.0 was maintained by the release of acid due to $HAuCl_4$ in the solution. This was followed by addition of 1 mL functionalized SiO_2 particles in water and was stirred at 75 °C for 10 min leading to the formation of the gold seeds with silica particles. The solution was centrifuged, washed with water and re-dispersed in 40 mL water. In step 2, K_2CO_3 (28 mg) in 100 mL milipore water and 1.5 mL of 25 mM gold solution were poured in 250 mL round bottom flask, stirred and aged in the dark for 12 h. In the final step 3, SiO_2@Au solution obtained in the step 1 and gold hydroxide solution from the step 2 were mixed and stirred for 10 min with (5.3 mM, 1.6 mL) $NaBH_4$ which leads to the formation of active SiO_2@Au core–shell NCs. The field emission scanning electron microscope (FESEM) images of the synthesized SiO_2@Au core–shell NCs were obtained and the mean diameter was determined to be 480 nm.

2.5. Characterization tools for Au NPs and SiO_2@Au NCs

The particle sizes in Au NPs and core–shell particles along with the morphological investigations have been studied using transmission electron microscopy (TEM), field FESEM and scanning electron microscopy (SEM) as per the requirements. The detection is also assessed using UV–vis absorption spectroscopy (for SPR) and SERS. Optical absorption spectra were recorded on Shimadzu UV-2401 spectrophotometer, USA. A Hitachi 2010 USA TEM, was used to investigate the particle morphology. SEM images were obtained using JEOLXL30 SEM, USA. FESEM images were obtained using Hitachi S-4800 USA microscope. Raman spectra were recorded with a Renishaw 2000 equipped with Ar^+ ion laser (λ=532 nm) and a charge-coupled device (CCD) as the detector (Renishaw Co., UK). Samples for Raman spectroscopy were prepared on ITO slides.

2.6. Sample preparation for SERS experiment

A series of different concentration of Cd^{2+} solutions 0.1, 1, 2, 5 and 10 ppm were prepared and have been used to detect based on nanomaterials dispersion. 5 mL of Cd^{2+} ions solutions each of 0.1, 1, 2, 5 and 10 ppm was mixed separately with 5 mL of Au NPs and also SiO_2@Au NCs dispersion in the different beakers. Each beaker solution was subsequently subjected to various characterizations. Throughout the experiment for doing the SERS activity, CV molecule substrate with concentration of 1.5×10^{-5} M was used. Then 50 μL of Au NPs and SiO_2@Au solutions of each were mixed separately with 500 μL of dye i.e. CV such that CV to nanomaterials (Au NPs or SiO_2@Au NCs) ratio is maintained as 10:1.

3. Results and discussion

The detection of Cd^{2+} ions has been reported in the literature using SERS active different metal NPs [16,18,20,23]. However, the development of simple, inexpensive and efficient sensor materials has always been desirable. In present method a facile, efficient and solution based colorimetric detection of Cd^{2+} ions is developed using speckled SiO_2@Au core–shell NCs which has not been reported in literature. Slightly less sensitive information is also possible with just Au NPs but speckled SiO_2@Au core–shell particles have been found to be much more sensitive than Au NPs and discussed in following sections.

3.1. TEM studies of AuNPs and SiO_2@Au NCs

Firstly, the size and morphology of gold nanoparticles and core–shell nanocomposites were determined using transmission electron microscopy. Fig. 1(a and b) represents the TEM images of spherical gold and silica nanoparticles respectively while Fig. 1 (c) shows the image of SiO_2@Au core–shell NCs. It was found that average gold nanoparticle size was ~30 nm and that of silica particles was ~420 nm which increased to ~480 nm for nanocomposites. Fig. 1(c) clearly indicates that the SiO_2@Au core–shell NCs synthesized were speckled particles i.e., they retain the gold particle size as was used in the formation of core–shell particles. However, they appear as separate particles with nanogaps between them and create a large number of adsorption sites for detection of foreign ions i.e. metal ions.

3.2. SPR studies of Au NPs and SiO_2@Au core–shell NCs

The surface plasmon resonance spectra for Au NPs and SiO_2@Au core–shell NCs solution have been depicted in Fig. 2. The SPR spectrum of Au NPs is sharper (a) as compared to that due to SiO_2@Au core–shell NCs (b) which may be attributed to reduced radiation damping for small particles. The SPR peak located at ca. 522 nm is due to Au NPs and that of core–shell particles at 541 nm. The peak slightly shifts to the red and becomes broader as the particle diameter increases. The broadening of SPR peak in SiO_2@Au core–shell NCs may be attributed to the enhanced radiation damping for large particles. It is important to note that the position of SPR peak of Au nanospheres depends on the dielectric constant of environment [37,42,49], thus, different solvent or adsorption of a capping agent onto the nanospheres may result in slight variation for the SPR peak position [42,49] and the same has been exploited in the present study.

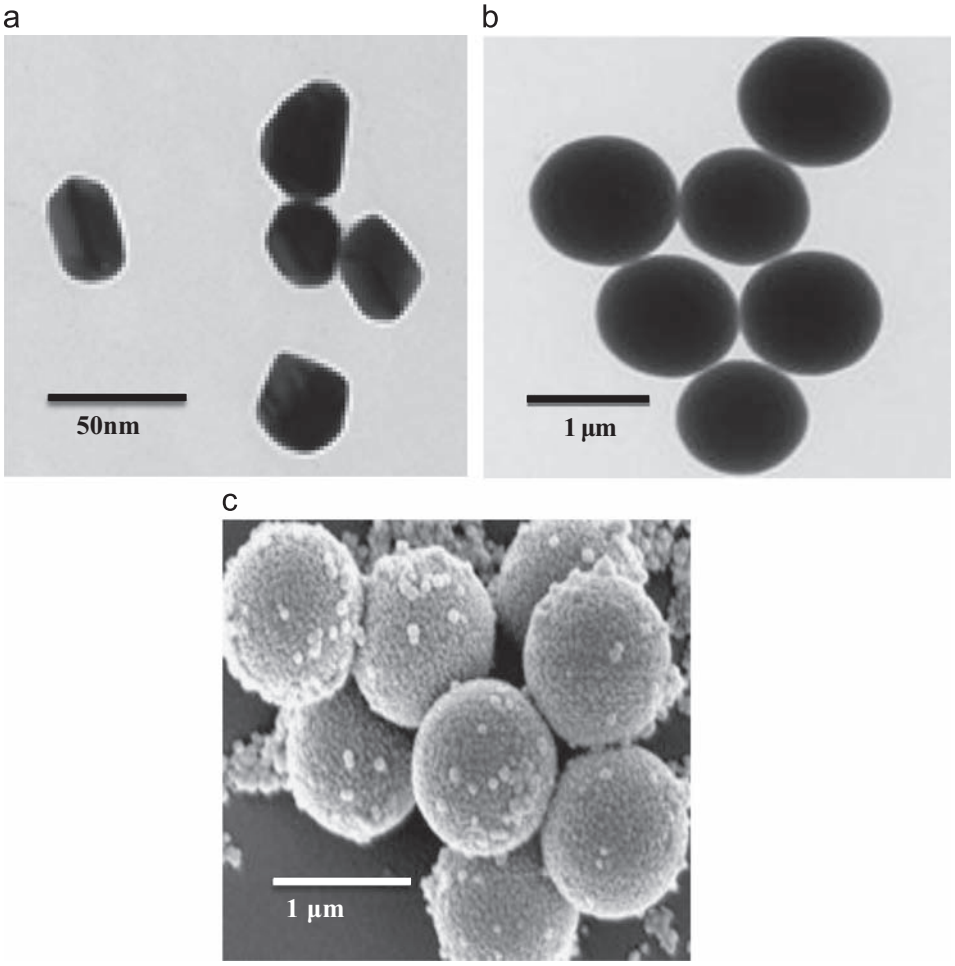

Fig. 1. Transmission electron microscopy images of (a) Gold nanoparticles (b) SiO_2 particles and (c) SiO_2@Au speckled silica-Au core–shell nanocomposites.

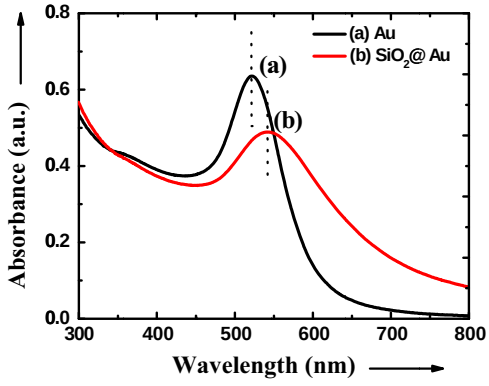

Fig. 2. Surface plasmon resonance spectra of (a) Au NPs (b) SiO_2@Au core–shell NCs.

3.3. Cd^{2+} ions detection and SEM studies

The colorimetric detection of Cd^{2+} ions was quite straight forward. Fig. 3(a) shows the effect of Cd^{2+} ions concentrations on Au NPs solution. Bottle no. 1 did not contain Cd^{2+} ions but only Au NPs solution and served as reference while bottle no. 2–6 contained 0.1, 1, 2, 5 and 10 ppm concentration of Cd^{2+} ions in increasing order respectively. It was noticed that there was no detectable change till 4th bottle which contained 2 ppm Cd^{2+} ions. At this concentration i.e. 2 ppm Cd^{2+} ions colour of the solution turned into greyish which indicated the detection limit of Au NPs technique. When same amounts of Cd^{2+} were added to the solutions of SiO_2@Au, the solution colour turned dark red even with 0.1 ppm concentration of Cd^{2+} ions as shown in bottle no. 2 in Fig. 3(b). Fig. 3(b) clearly shows that with addition of 1 ppm concentration of Cd^{2+} ions, the colour turned even darker while with 2 ppm Cd^{2+} ions the solution became colourless. Hence, Cd^{2+} concentrations more than 2 ppm cannot be quantitatively analyzed by SiO_2@Au NCs and thus limits the detection range from 100 to 2000 ppb (0.1 to 2 ppm). Also continued addition of 5 and 10 ppm Cd^{2+} ions, SiO_2@Au NCs solution did show a color change relative to the Cd-free solution i.e. became colourless in bottle no. 5 and 6 (Fig. 3b). Thus the technique using SiO_2@Au NCs is quantitative between 100 to 2000 ppb (0.1 to 2 ppm) while effective but non-quantitative above upto 10,000 ppb (10 ppm) as we have studied in present investigation. In brief, SiO_2@Au nanocomposites are able to detect as low as 100 ppb (0.1 ppm) while Au NPs is able to detect Cd^{2+} as low as 2000 ppb (2 ppm) and the same are clearly shown in Fig. 3.

The colorimetric changes in Au NPs and SiO_2@Au NCs solutions on addition of different concentration of Cd^{2+} ions into them (Fig. 3) clearly shows that for Au NPs solution there was no rapid colorimetric change as compared to SiO_2@Au NCs solution and the same were observed by UV–vis spectra. The same has also been supplemented by the changes in the surface plasmon resonance peaks as shown in Fig. 4(a and b) which represents SPR spectra of Au NPs and SiO_2@Au NCs solution respectively in the presence of varied amounts of Cd^{2+} ions.. The changes in colour due to Cd^{2+} ions were accompanied by the changes in the SPR spectra. Change in SPR peak started appearing at 2 ppm as the colour changes from wine red but at high ppm level the colour of the solutions changes

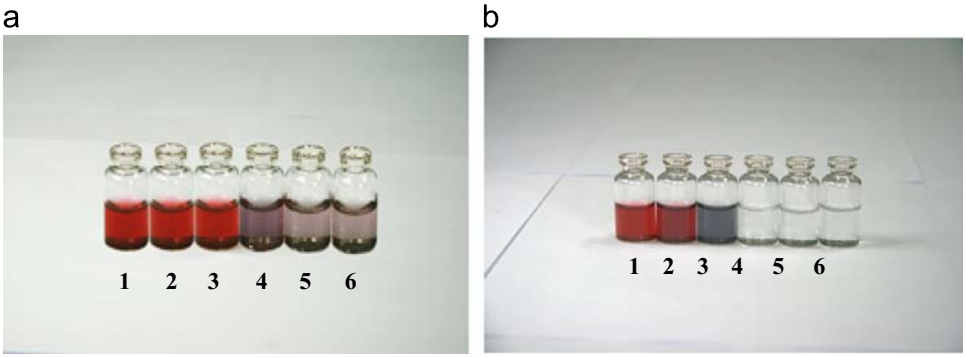

Fig. 3. Visual detection of Cd^{2+} ions by addition of 0.0, 0.1, 1, 2, 5 and 10 ppm Cd^{2+} ions (correspond to 1–6 in increasing order) respectively in (a) Au NPs solution and (b) speckled silica-gold core–shell solution.

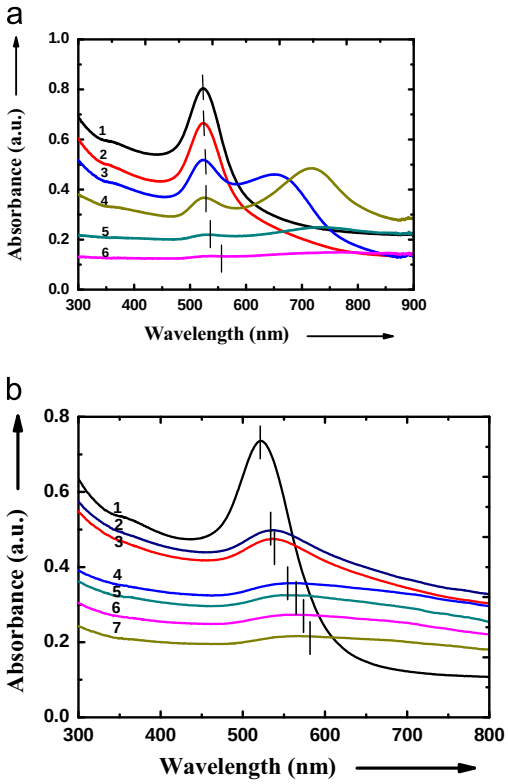

Fig. 4. (a) Changes in surface plasmon resonance peaks with (1) Au NPs solution as reference [2] Au NPs+0.1 ppm Cd^{2+} (3) Au NPs+1 ppm Cd^{2+} (4) Au NPs+2 ppm Cd^{2+} (5) Au NPs+5 ppm Cd^{2+} and (6) Au NPs+10 ppm Cd^{2+}. (b) Changes in surface plasmon resonance peaks with (1) Au NPs solution as reference [2] SiO_2@Au solution (3) SiO_2@Au+0.1 ppm Cd^{2+} (4) SiO_2@Au+1 ppm Cd^{2+} (5) SiO_2@Au+2 ppm Cd^{2+} (6) SiO_2@Au+5 ppm Cd^{2+} and (7) SiO_2@Au+10 ppm Cd^{2+}.

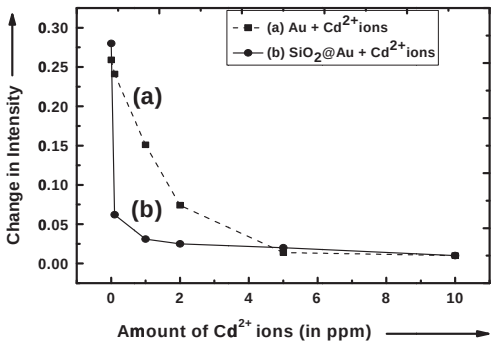

Fig. 5. Variation in the intensity of the SPR peaks at 522 nm for Au NPs and 541 nm for SiO_2@Au NCs with Cd^{2+} ion addition in the range of 0.1–10 ppm.

to blue and in a linear fashion which also accounts for the appearance of the peaks beyond 600 nm in Fig. 4(a). These may be due to change in shape of particles from spherical to rod shape which indicates longitudinal mode of Au nanorods.

The variation in the intensity of SPR peaks for Au NPs at 522 nm and SiO_2@Au NCs at 541 nm due to Cd^{2+} ions addition in the range of 0.1–10 ppm is shown in Fig. 5. The changes in the intensity noticed were quite consistent with colour changes shown in Fig. 3(a and b) where changes in case of SiO_2@Au solution occur at lower concentration of Cd^{2+} ions as compared to that of Au NPs solution.

The changes in SPR peak intensities are often attributed to changes in the optical properties of the medium in which metal particles are dispersed [23,37,42,49]. The changes in the dielectric constant or aggregation of particles may be responsible for the changes in SPR spectra and intensities [23,37,42,49]. In addition, the aggregation of Au NPs lead to a pronounced colour transition from red to purple which is due to plasmonic coupling between particles [18,19,42]. In order to verify this observation, SEM images after the addition of 0.1 ppm of Cd^{2+} ions separately to Au NPs solution and SiO_2@Au solutions were taken and are shown in Fig. 6 (a) and (b), respectively.

Fig. 6(a and b) clearly shows different degree of aggregation in two samples. Fig. 6(a) also shows that the aggregation in Au NPs solution is less compared to that in SiO_2@Au as shown in Fig. 6(b). The surface of nanocomposite material is treated as negatively charged and even electron density increases due to dielectric SiO_2 core. Thus on addition of positively charged Cd^{2+} ions into negatively charged nano-composite solution induces aggregation of colloidal particles or decrease inter-particle distance. The difference in aggregation may be attributed to change in the dielectric of the surrounding environment [23,37,42,49]. Moreover, the Au NPs in Fig. 6(a) are aggregated in a linear fashion which also could account for the appearance of peaks beyond 600 nm in Fig. 4(a). These are like longitudinal mode of Au nanorods [23,37,43].

3.4. SERS study on Cd^{2+} ions interaction with Au NPs or SiO_2@Au core–shell NCs

The interaction between Cd^{2+} ions and Au NPs or SiO_2@Au core–shell NCs was further investigated using Raman spectroscopy, an excellent technique to investigate the interactions at molecular level. The SERS spectra of Au NPs and SiO_2@Au core–shell NCs are shown in Fig. 7(a) and (b) respectively. It was obtained by mixing nanoparticles with 10^{-4} M solution of CV molecule and 200 μL of this mixture was dropped on ITO for 12 h drying. The sensitivities of the Au NPs and SiO_2@Au core–shell NCs surfaces however were extremely low towards SERS and thus no

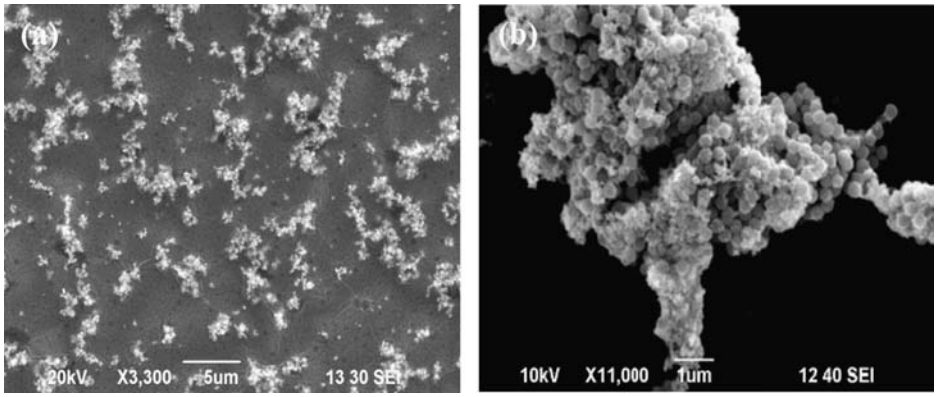

Fig. 6. Scanning electron microscopy images after the addition of 0.1 ppm Cd^{2+} ions to (a) Au NPs solution and the same amount in (b) SiO_2@Au core–shell NCs solution.

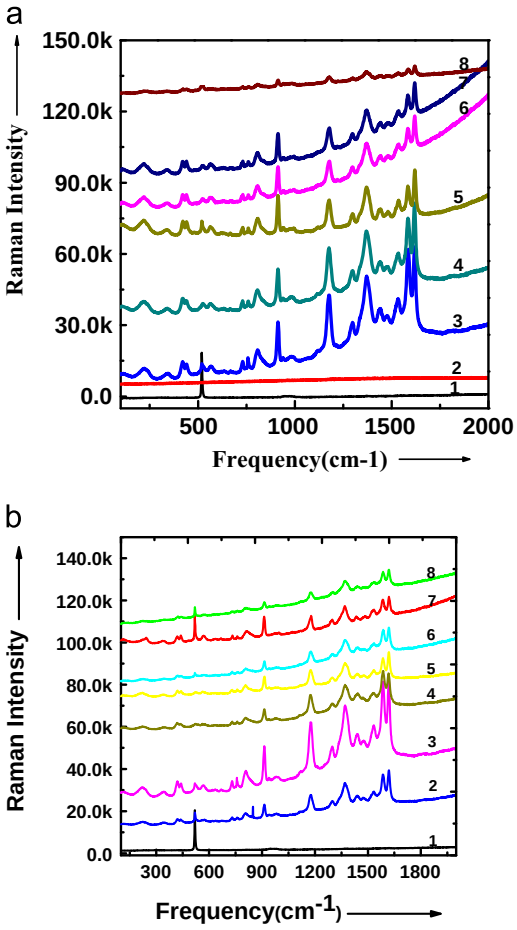

Fig. 7. (a) SERS spectra using CV molecule (10^{-4} M) concentration and 0.05% laser power and λ=532 nm: (1) CV (2) Au NPs (3) CV+Au NPs (4) CV+Au NPs+0.1 ppm Cd^{2+} (5) CV+Au NPs+1 ppm Cd^{2+} (6) CV+Au NPs+2 ppm Cd^{2+} (7) CV+Au NPs+5 ppm Cd^{2+} and (8) CV+Au NPs+10 ppm Cd^{2+} ions. (b). SERS spectra using CV molecule (10^{-4} M) concentration and 0.05% laser power and λ=532 nm: (1) CV (2) CV+Au NPs (3) CV+SiO_2@Au (4) CV+SiO_2@Au+0.1 ppm Cd^{2+} (5) CV+SiO_2@Au+1 ppm Cd^{2+} (6) CV+SiO_2@Au+2 ppm Cd^{2+} (7) CV+SiO_2@Au +5 ppm Cd^{2+} and (8) CV+SiO_2@Au+10 ppm Cd^{2+} ions.

detectable signal of Au NPs or SiO_2@Au on ITO surfaces could be observed. In order to detect the Raman spectrum from single molecules, it was necessary to take advantage of the additional boost up in intensity provided by a molecular resonance, and therefore dye molecule crystal violet (CV) was employed. Therefore both the surfaces (Au NPs and SiO_2@Au) were coated with CV molecules. Interestingly when CV molecules alone were spread on ITO substrates they gave signals only at around 500 cm^{-1}. However with Au NPs or SiO_2@Au core–shell NCs covered surfaces, there was a large enhancement of CV molecule signal and a number of peaks appeared as shown in Fig. 7(a) (no. 3) and in 7 (b) (no. 2) and the similar observation has also been reported in the literature by Dasary et al. [42].

When Cd^{2+} ions in varied concentrations in the range 0.1 to 10 ppm were added on these substrates; it was noticed that in case of Au NPs with CV molecules covered surface the peaks appeared at 1620 cm^{-1}(sh), 1585 cm^{-1}(s), 1532 cm^{-1}(s), 1473 cm^{-1}(m), 1443 cm^{-1}(s), 1375 cm^{-1}(s), 1302 cm^{-1}(w), 1214 cm^{-1}(sh), 1175 cm^{-1}(s), 986 cm^{-1}(vw), 916 cm^{-1}(s), 813 cm^{-1}(w), 764 cm^{-1}(w) and 525 cm^{-1}(w) for Au NPs and the intensities decreased on increasing concentration of Cd^{2+} ions as shown in Fig. 7(a) spectra 3–8. On SiO_2@Au covered surface, CV molecules exhibited peaks at 1620 cm^{-1}(sh), 1586 cm^{-1}(s), 1537 cm^{-1}(w), 1482 cm^{-1}(w), 1438 cm^{-1}(s), 1375 cm^{-1}(s), 1297 cm^{-1}(w), 1180 cm^{-1}(s), 979 cm^{-1} (vw), 916 cm^{-1}(s), 852 cm^{-1}(w), 754 cm^{-1}(vw) and 515 cm^{-1}(w) and sharply decreased with Cd^{2+} concentration (s, strong; m, medium; w, weak; vw, very weak and sh, shoulder). The decrease in the intensity for Au NPs peaks were clearly noticeable when 2 ppm Cd^{2+} ions were present while for SiO_2@Au at 0.1 ppm and the same observation was found during the study of the variation of the intensity of SPR peaks for Au NPs and SiO_2@Au NCs as shown in Fig. 5.

It was observed that Au NPs or SiO_2@Au core–shell NCs coated ITO substrates did not give any detectable Raman signal. Similarly, CV molecules also did not show any Raman signal except at around 500 cm^{-1}. However when CV molecules were dispersed on Au NPs or SiO_2@Au covered ITO surfaces, various vibration modes were appeared with large enhancement of intensities (Fig. 7) but with the addition Cd^{2+} ions, the signal of CV molecules got suppressed. The reduction in the intensities consistent with the SPR observations i.e. SiO_2@Au NCs is more sensitive as compared to Au NPs (Section 3.3, cf. Fig. 5). The SERS study concluded that SiO_2@Au surface attracts a greater number of crystal violet (CV) substrate and it increases number of hot spots through aggregation, providing a significant enhancement of the Raman signal intensity than is obtained in Au NPs [41].

3.5. Selectivity/application and comparison

The selectivity for the target analyte is the most important characteristics of a colorimetric sensor. To determine the selectivity of the colorimetric assay of Cd^{2+} using Au NPs in the presence of several environmental relevant and potentially competing ions such as Pb^{2+}, Zn^{2+}, Fe^{2+} and K^{+}, 2 ppm concentration of each of these metal ions were added into Au NPs solution. No effects of these metals were observed while the colour change in presence

Table 1
A comparison of the proposed method with other methods for detection of Cd^{2+} ions.

Sensors for the detection of Cd^{2+}	Detection limit, material used, comments	Ref.
Turn-on fluorescent InP nanoprobe for detection of cadmium ions	12 μM; InP nanoprobe; visualized detection, high selectivity and sensitivity	[66]
Label-free colorimetric detection of cadmium ions in rice samples using gold nanoparticles	10 μM in rice samples, Au NPs accompanied by glutathione, easily aggregate in a high [NaCl] solution	[67]
SERS-Active nanoparticles for sensitive and selective detection of Cd^{2+}	25 μM, SERS-active 41 nm Au NPs, sensitive and selective detection but uses a layer of Cd^{2+}-chelating polymer	[68]
Micro fluidic device for Cd^{2+} detection using gold nanoparticles	10 μM, Au NPs colloid, power-free and reusable, colorimetric assay	[69]
Plasmonic detection of Cd^{2+} ions using surface-enhanced Raman scattering active core–shell nanocomposite	100 ppb, SiO_2@Au NCs, shows high selectivity and sensitivity, necked eye detection	Present work

of Cd^{2+} at 2 ppm (2000 ppb) was quite easily observed by naked eye.

Similarly, the colorimetric response of SiO_2@Au core–shell NCs in the presence Cd^{2+}, Pb^{2+}, Zn^{2+}, Fe^{2+} and K^{+} were tested by adding of 0.1 ppm (100 ppb) as well as 1 ppm (1000 ppb) concentrations of these metal ions separately into SiO_2@Au NCs solution. No effects of these metals were observed while the colour changes in presence of 0.1 ppm as well as 1 ppm Cd^{2+} were easily observed by naked eye and also confirmed by UV–vis spectra of the respective solutions. In terms of visual observation and real application to water samples, the colour of SiO_2@Au NCs solution changes from wine red to blue only in presence Cd^{2+}. Thus it is extremely easy to detect Cd^{2+} and it distinguish other metal ions using SiO_2@Au NCs.

The proposed method was also compared with other existing methods for detection of Cd^{2+} ions as shown in Table 1 [66–69]. The proposed method has its limitations for water analysis since the detection limit is 20 times higher than the Environmental Protection Agency limit. The proposed method using SiO_2@Au NCs shows high selectivity and sensitivity, naked eye detection upto 100 ppb Cd^{2+} in water samples. Hence the synthesized Au NPs and SiO_2@Au core–shell NCs can play an important role as a surface plasmon resonance based sensor to detect the concentration of Cd^{2+} in the range of 100–2000 ppb.

4. Conclusions

The detection of Cd^{2+} ions in water was studied using Au NPs and SiO_2@Au core–shell NCs with core of 420 nm and shell of ~30 nm thickness. It was observed that both Au NPs and SiO_2@Au core–shell NCs solutions exhibit excellent colour sensitivity towards Cd^{2+} ions. However, SiO_2@Au core–shell NCs have 100 ppb (0.1 ppm) sensitivity for the detection of Cd^{2+} ions as compared to 2000 ppb (2 ppm) sensitivity with Au NPs. Our study concluded that speckled SERS active core–shell particles of SiO_2@Au can be reliably synthesized through stringently controlled chemical synthesis and is 20 fold more sensitive probes, for the detection of Cd^{2+} ions as compared to Au NPs, with high selectivity and sensitivity.

Acknowledgments

This research was supported by foundation of Beijing key laboratory, China. ST and PK would like to thank Capital Normal University, Beijing, China for the travel support. DK is thankful to the University Grant Commission (UGC), New Delhi, India for financial assistance via grant no. F.No.39-734/2010 (SR). The authors would like to acknowledge Prof. S.K. Kulkarni for her support and encouragement.

References

[1] L. Järup, Br. Med. Bull. 68 (2003) 167–182.
[2] R. Singh, N. Gautam, R. Gupta, Indian J. Pharmacol. 43 (2011) 246–253.
[3] F.M. Strong, Nutr. Rev. 32 (1974) 225–231.
[4] S. Shirahata, T. Hamasaki, K. Haramaki, T. Nakamura, M. Abe, H. Yan, T. Kinjo, N. Nakamichi, S. Kabayama, K. Teruya, in: BioMed Central Proceedings 5 (2011) 18-20.
[5] H. Jansa, Q. Huo, Chem. Soc. Rev. 41 (2012) 2849–2866.
[6] O. Barbier, G. Jacquillet, M. Tauc, M. Cougnon, P. Poujeol, Nephron Physiol. 99 (2005) 105–110.
[7] J. Coresh, D. Byrd-Holt, B.C. Astor, J.P. Briggs, P.W. Eggers, D.A. Lacher, T. H. Hostetter, J. Am. Soc. Nephrol. 16 (2005) 180–188.
[8] C.A. Pedro, M.S.S. Santos, S.M.F. Ferreira, S.C. Gonçalves, Mar. Environ. Res. 92 (2013) 197–205 (and references cited therein).
[9] EC, 2001. Decision No. 2455/2001/EC of the European Parliament and of the Council of 20 November 2001 establishing the list of priority substances in the field of water policy and amending Directive 2000/60/EC. Off. J. Eur. Commun. L 331, 1–5.
[10] USA Environmental Protection Agency (USA EPA), 2001. 2001 update of Ambient Water Quality Criteria for Cadmium. EPA-822-R-01-001.
[11] OSPAR Commission, Review Statement for the OSPAR Background Document on Cadmium, 2010. Available at ⟨http://www.ospar.org/documents/dbase/publications/p00509/p00509_cd_review_statement.pdf⟩ (Accessed on 2 June 2014).
[12] P.H.C. Camargo, K.G. Satyanarayana, F. Wypych, Mater. Res. 12 (2009) 1–39.
[13] M.M. Kin, S. Nair, J.B. Veluru, M. Rajendiran, S. Ramakrishan, Energy Environ. Sci. 5 (2012) 8075–8109.
[14] X. Chen, X. Cheng, J.J. Gooding, Analyst 137 (2012) 2338–2343.
[15] Y. Kim, R.C. Johnson, J.T. Hupp, Nano Lett. 1 (2001) 165–167.
[16] J. Yin, T. Wu, B.J. Song, Q. Zhang, S. Liu, R. Xu, H. Duan, Chem. Mater. 23 (2011) 4756–4764.
[17] D. Liu, Z. Wang, X. Jiang, Nanoscale 3 (2011) 1421–1433.
[18] M.S. Bootharaju, T. Pradeep, J. Phys. Chem. C 114 (2010) 8328–8336.
[19] Y. Xue, H. Zao, Z. Wu, X. Li, Y. He, Z. Yuan, Analyst 136 (2011) 3725–3730.
[20] L. Zhang, W.D. Li, W. Song, L. Shi, Y. Li, T.Y. Long, Sensors J. IEEE 10 (2011) 1583–1588.
[21] A.R.M. Salcedo, F.B. Sevilla, Philippine Sci. Lett. 6 (2013) 90–96.
[22] Z. Wang, J.H. Lee, Y. Lu, Adv. Mater. 20 (2008) 3263–3267.
[23] S. Thatai, P. Khurana, J. Boken, S. Prasad, D. Kumar, Microchem. J. 116 (2014) 62–76.
[24] V.V. Srdic, B. Mojic, M. Nikolic, S. Ognjanovic, Process. Appl. Ceram. 7 (2013) 45–62.
[25] D.W. Li, W.L. Zhai, Y.T. Li, Y.T. Long, Microchim Acta 181 (2014) 23–43.
[26] R.A. Halvorson, P.J. Vikesland, Environ. Sci. Technol. 44 (2010) 7749–7755.
[27] W.E. Smith, Chem. Soc. Rev. 37 (2008) 955–964.
[28] R.A. Alvarez-Puebla, L.M. Liz-Marzan, Energy Environ. Sci. 3 (2010) 1011–1017.
[29] M.K. Fan, G.F.S. Andrade, A.G. Brolo, Anal. Chim. Acta 693 (2011) 7–25.
[30] M.V. Limaye, S.B. Singh, S.K. Date, R.S. Gholap, S.K. Kulkarni, Mater. Res. Bull. 44 (2009) 339 (-334).
[31] S.C. Erwin, L. Zu, M.I. Haftel, A.L. Efros, T.A. Kennedy, D.J. Norris, Nature 436 (2005) 91–94.
[32] A. Ethiraj, N. Hebalkar, S.K. Kulkarni, R. Pasricha, J. Urban, M. Schmitt, W. Kiefer, L. Weinhardt, S. Joshi, R. Fink, C. Heske, C. Kumpf, E. Umbach, J. Chem. Phys. 118 (2003) 8945–8953.
[33] S.A. Kalele, A.A. Kundu, S.W. Gosavi, N.D. Deobagkar, D.D. Deobagkar, S. K. Kulkarni, Small 2 (2006) 335–338.
[34] J.L. West, N.J. Halas, Annu. Rev. Biomed. Eng. 5 (2003) 285–292.
[35] M. Fang, T.T. Volotinen, S.K. Kulkarni, L. Belova, K.V. Rao, J. Appl. Phys. 108 (2010) 103501–103507.
[36] S.A. Kalele, S.S. Ashtaputre, N.Y. Hebalkar, S.W. Gosavi, D.N. Deobagkar, D.D. Deobagkar, S.K. Kulkarni, Chem. Phys. Lett. 404 (2005) 136–141.
[37] P. Khurana, S. Thatai, P. Wang, P. Lihitkar, L. Zhang, Y. Fang, S.K. Kulkarni, Plasmonics 8 (2013) 185–191 (and references cited therein).
[38] S. Kalele, S.W. Gosavi, J. Urban, S.K. Kulkarni, Curr. Sci. 91 (2006) 1038–1052.
[39] I. Pastoriza-Santos, D. Gomez, J. Perez-Juste, L.M. Liz-Marzan, P. Mulvaney, Phys. Chem. Chem. Phys. 6 (2004) 5056–5060.

[40] B.J. Jankiewicz, D. Jamiola, J. Choma, M. Jaroniec, Adv. Colloid Interface 170 (2012) 28–47.
[41] D.K. Lim, K.S. Jeon, J.H. Hwang, H. Kim, S. Kwon, Y.D. Suh, J.M. Nam, Nat. Nanotechnol. 6 (2011) 452–460.
[42] S.S.R. Dasary, P.C. Ray, A.K. Singh, T. Arbneshi, H. Yu, D. Senapati, Analyst 138 (2013) 1195–1203.
[43] S. Thatai, P. Khurana, S. Prasad, D. Kumar, Microchem. J. 113 (2014) 77–82 (and references cited therein).
[44] H.S. Santos, G.M. de França, E.C. Romani, D.G. Larrudé, A.L.M.C. da Cunha, R.Q. Aucélio, A.R. da Silva, Microchem. J. 116 (2014) 206–215.
[45] E. de B. Santos, E.C.N.P. Lima, C.S. de Oliveira, F.A. Sigoli, I.O. Mazali, Anal. Methods 6 (2014) 3564–3568.
[46] D. Huang, T. Hu, N. Chen, W. Zhang, J. Di, Anal. Chim. Acta 825 (2014) 51–56.
[47] M.O. Noor, U.J. Krull, Anal. Chim. Acta 825 (2014) 1–25.
[48] M.-C. Estevez, M.A. Otte, B. Sepulveda, L.M. Lechuga, Anal. Chim. Acta 806 (2014) 55–73.
[49] B. Saute, R. Premasiri, L. Ziegler, R. Narayanan, Analyst 137 (2012) 5082–5087.
[50] H. Wang, Z. Wang, M. Ye, S. Zong, M. Li, P. Chen, X. Ma, Y. Cui, Talanta 119 (2014) 144–150.
[51] P.A. Mosier-Boss, M.D. Putnam, Anal. Chim. Acta 801 (2013) 70–77.
[52] F.P. Zamborini, L. Bao, R. Dasari, Anal. Chem. 84 (2012) 541–576.
[53] G.P. Pandey, A.K. Singh, L. Deshmukh, S. Prasad, L.J. Paliwal, A. Asthana, S.B. Mathew, Microchem. J. 113 (2014) 83–89.
[54] R.M. Naik, S. Prasad, B. Kumar, S.B.S. Yadav, A. Asthana, M. Yoshida, Microchem. J. 111 (2013) 108–115.
[55] R.M. Naik, S. Prasad, B. Kumar, V. Chand, Microchem. J. 111 (2013) 97–102.
[56] V. Chand, S. Prasad, J. Hazardous Mater. 165 (2009) 780–788.
[57] S. Prasad, R.M. Naik, A. Srivastava, Spectrochim. Acta Pt. A 70 (2008) 958–965.
[58] S. Prasad, Microchem. J. 85 (2007) 214–221.
[59] S. Prasad, Anal. Chim. Acta 540 (2005) 173–180.
[60] R. Prasad, R. Kumar, S. Prasad, Anal. Chim. Acta 646 (2009) 97–103.
[61] S. Prasad, T. Halafihi, Microchim. Acta 142 (2003) 237–244.
[62] S. Prasad, P.C. Nigam, Talanta 38 (1991) 627–630.
[63] C. Graf, D.L.J. Vossen, A. Imhof, A.V. Blaaderen, Langmuir 19 (2003) 6670–6693.
[64] V.G. Pol, A. Gedanken, J. Calderon-Moreno, Chem. Mater. 15 (2003) 1111–1118.
[65] W. Stöber, A. Fink, E. Bohn, J. Colloid Interface Sci. 26 (1968) 62–69.
[66] Y. Zhang, Z. Zhang, D. Yin, J. Li, R. Xie, W. Yang, ACS Appl. Mater. Interfaces 5 (2013) 9709–9713.
[67] Y. Guo, Y. Zhang, H. Shao, Z. Wang, X. Wang, X. Jiang, Anal. Chem. 86 (2014) 8530–8534.
[68] J. Yin, T. Wu, J. Song, Q. Zhang, S. Liu, R. Xu, H. Duan, Chem. Mater. 23 (2011) 4756–4764.
[69] S. Al-Lami, A. Faisal, J.F. Hamodi, Q. Aljimily, H. Ibrahim, F. Hamood, A. Hussein Nagm, G.P. Li, Eng. Technol. J. 32 (2014) 540–549.